Patterned Growth of ZnO Nanorod Arrays on a Large-Area Stainless Steel Grid

Xiang Yu Xu, Hong Zhou Zhang, Qing Zhao, Yao Feng Chen, Jun Xu, and Da Peng Yu*

Electron Microscopy Laboratory and State Key Laboratory for Mesoscopic Physics, School of Physics, Peking University, Beijing 100871, People's Republic of China

Received: July 23, 2004; In Final Form: October 21, 2004

Large-area ZnO nanorod arrays have been synthesized successfully on a stainless steel grid at a mild growth temperature of around 400 °C. The as-grown ZnO nanorods have uniform diameters of about 30−50 nm with ∼5 nm tips. Patterned growth can be realized by engineering the shape of the grid in the growth. Photoluminescence demonstrates a sharp strong UV peak and a broad green band. The growth method provides a promising way of producing nanorod arrays with good controllability in patterns and morphologies, which will be critical in potential application such as high-efficiency filtering and catalysts.

Introduction

With the extensive applications of bulk or film ZnO in various areas, such as gas sensors,[1] power devices,[2] UV-light-emitting diodes,[3] photocatalysts,[4] and CMOS-chip-integrated microphones,[5] and the appearance of its good properties with the reduction of the size of bulk ZnO to nanoscale,[6] there is overwhelming interest in the research field on how to fabricate ZnO nanostructures in a controllable way. Recently, many methods have been developed for this aim, such as physical evaporation (PE),[7] chemical vapor transport (CVT),[8] molecular beam epitaxy (MBE),[9] physical vapor deposition (PVD),[10] metal−organic chemical vapor deposition (MOCVD),[11] and aqueous solution deposition.[12,13] For example, the soft wet chemical route can really obtain highly aligned ZnO nanotip arrays at a remarkably low temperature[14] but needs a complicated reaction process. However, the morphologies of these ZnO quasi-one-dimensional nanostructures are strongly dependent on particular synthesis methods. Much effort has been devoted to improving the controllability of the fabrication, including the morphology of individual nanowires or nanorods, alignment between nanowires or nanorods, and selective growth on specific substrates. Among these methods, both the template technique[13] and self-assembly[15] are successful in aligning the ZnO nanowires, and selective growth is usually conducted by patterning the catalyst layer.[9,16] But it is difficult to realize selective growth in the case of self-assembly. On the contrary, the patterned catalyst method usually lacks alignment control. What is more, most of these methods generally produce ZnO nanostructures on silicon or sapphire substrates on the microscale level in the laboratory, presenting a limit toward the road of large-scale industrial production. Therefore, it is imperative to develop an alternative method to tackle the problem from the science and technology point of view. In this paper, we report the patterned growth of well-aligned ZnO nanorod arrays on a large-area stainless steel grid at a relatively mild temperature around 400 °C via vapor-phase growth. The function of the grid is discussed in detail. To the best of our knowledge, well-aligned ZnO nanorod arrays were synthesized on a novel substrate, a steel grid, for the first time, which gives more possibility in controlling gas flow and diverse pattern designs by changing the grid pore size and the grid shape needed. Using a stainless steel grid as substrate suggests controllable growth over a macroscale area. The process developed in this work offers a novel and efficient approach to realize selective growth and good alignment of the nanorods on a large-area substrate at the same time. It is also important to point out that this new route may be extended to the controllable formation of a wide variety of other ordered nanostructures.

* To whom correspondence should be addressed. E-mail: yudp@pku.edu.cn.

Experimental Section

Different from conventional physical evaporation, the substrate and its positioning to the source were cautiously considered in the growth method. A stainless steel grid with a grid period of 20 μm and a size of 1 cm × 5 cm was used as the substrate. A 10 nm thick Au film was first deposited on one side of the grid by E-beam-assisted evaporation. Then, the grid was placed onto a quartz boat that was filled with Zn powders (purity 99.999%). The Au-coated side of the grid was placed to face the Zn powders. The distance between the surface of the source and the grid was about 2−5 mm. The boat was then located at the center of a quartz tube, which was put into a tube furnace later. Another quartz boat with selenium powders was placed into the quartz tube near the gas inlet of the system. The precise locations of the boats were determined by the temperature requirements and the temperature distribution inside the quartz tube. During the growth, a constant Ar flow of 100 sccm and a minimum amount of oxygen were introduced into the system from one end of the tube (i.e., the gas inlet), and a mechanical pump vacuumed the system from the other end to maintain a pressure of about 100 Pa inside the tube. The temperatures of the Zn and Se sources were then elevated to 400 and 350 °C at a rate of 20 °C/min, respectively. The reaction lasted for about 45 min. After cooling, the Au-coated side of the grid showed a yellow cyan color. X-ray diffraction (XRD) was used to identify the phase of the as-grown samples. The surface morphology was investigated by a field emission Strata DB235-FIB working in scanning electron microscopy (SEM) mode. A transmission electron microscope (Tecnai F30) was used to analyze the structure and composition of the as-grown samples (the transmission electron microscopy (TEM) sample was scratched from the Au-coated side of the grid by a sharp

10.1021/jp046725x CCC: $30.25
Published on Web 01/12/2005

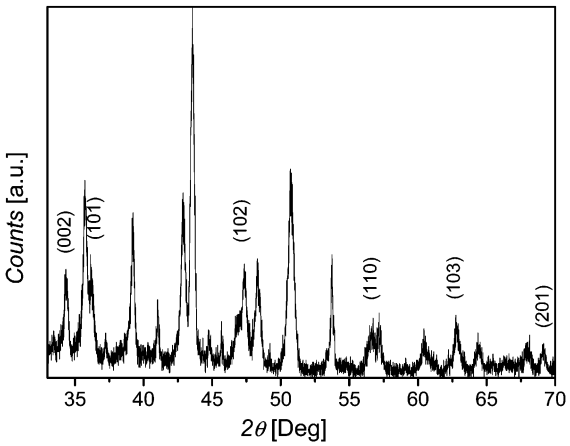

Figure 1. XRD pattern of the as-grown products. The indexed peaks correspond to the wurtzite ZnO structure, while other peaks correspond to the Au-coated stainless steel grid.

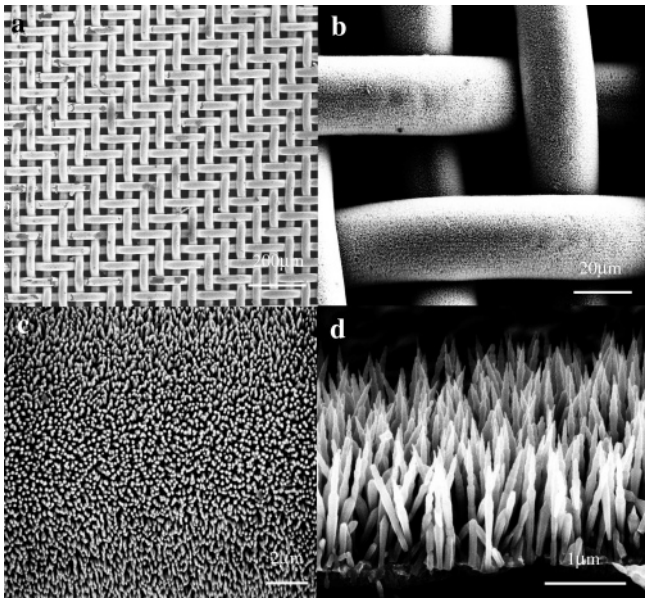

Figure 2. (a) A low-magnification SEM image showing the aligned nanorods covering the whole area of the steel grid. The grid pores are clearly visible. (b) Magnified SEM image of (a). The bright stripes are the grid frames, and they are covered with a flocky layer of ZnO nanorod arrays. (c) Representative image at a higher magnification showing the general morphology of the well-aligned ZnO nanorod arrays grown perpendicular to the surface of a single stainless steel grid. (d) A magnified cross-sectional SEM view of the flocky layer, which was peeled off from the grid framework, showing the good alignment and uniformity of the ZnO nanorod arrays.

forceps). The photoluminescence (PL) spectra were measured using a He−Cd laser of 325 nm wavelength at room temperature.

Results and Discussion

The XRD pattern of the as-grown samples is shown in Figure 1. The peaks without indexing arise from the Au-coated grid, which is elucidated by measurements of the XRD pattern of the grid before the growth. The indexed peaks correspond to ZnO with a wurtzite structure. The remaining peaks arise from the supporting stainless steel grid.

High uniform coverage of the densely packed array of ZnO nanorods was observed using SEM. The SEM images shown in Figure 2 are representative morphologies of the entire grid surface. Figure 2a shows a very low magnification SEM image taken from one section of the whole 5 cm^2 grid. Grid pores are clearly visible. The nanorods uniformly covered all the cylindrical grid frameworks we designed intentionally in advance in a large area up to square millimeters. The magnified SEM image of Figure 2a is shown in Figure 2b. The white bright stripes are the frameworks of the grid. It can be clearly seen that the surface of the grid was evenly covered with a flocky layer. A higher magnification image in Figure 2c shows the general morphology of the well-aligned ZnO nanorod arrays grown perpendicular to the surface of one stainless steel grid framework. The high density and alignment of the covered nanorod arrays can be observed in the image. Figure 2d is a tilted higher magnified SEM image of a flocky layer peeled off from the grid framework, showing that the nanorods have uniform morphologies and quite sharp tips. The nanorods are 1−2 μm in length and have a large aspect ratio.

TEM was employed to further investigate the structural details of the nanorods. The typical TEM morphology of the nanorods is shown in Figure 3a. Despite the fact that the preparation of the TEM samples could damage the alignment to some degree, it can still be perceived distinctly in the image. The nanorods have shrinking necks with sharp tips and have an average diameter of 30−50 nm. The high-resolution TEM (HRTEM) image shown in Figure 3b reveals that the radius of curvature of the tip is only ∼5 nm, which is beneficial in applications in field emission.[17] Atomic planes with an interplanar spacing of 0.5207 nm are continuous throughout the whole image, indicating the growth direction is [0001] and the nanorods are single crystalline in nature. EDS results (Figure 3c) show only Zn and O peaks (Cu and C peaks arise from the TEM grid and the carbon supporting membrane) for the nanorods. No Se element was detected from the nanorods within experimental limits. XRD, EDS, and microscopic results demonstrate that the as-grown samples are single-crystalline ZnO nanorod arrays.

The room-temperature photoluminescence spectrum recorded from the as-grown ZnO nanorod arrays is shown in Figure 4. A sharp and strong UV peak is centered at 3.31 eV (375 nm in wavelength), and a weak broad green band is found in the range of 2.07−2.92 eV (425−600 nm in wavelength). UV band emission of the ZnO nanorod arrays can be assigned to the emission from the free exciton under low excitation intensity.[6] It has been proved that the singly ionized oxygen vacancy is responsible for the green emission in ZnO.[18] The strong UV emission and the weak green band in the PL spectrum indicate that the ZnO nanorod arrays have a good crystal quality, which is consistent with the TEM results. The supporting metal grid has no obvious effect on the optical properties of the nanorods, which suggests that there is no significant metal diffusion in the nanorods during the growth process.

The high alignment of the ZnO nanorod arrays is a direct result of the confinement of the reactant vapor by the grid. The gas flow surrounding the grid during the growth can be understood as follows.[19] The Knudsen number (Kn) is the criterion for distinguishing the flow regimes, $Kn = D_p/\lambda_{mfp}$, where D_p and λ_{mfp} are the characteristic dimensions of the reaction chamber and the gas mean-free path, respectively. Taking the parameters of our experiment, we can make a simple estimation of Kn. The gas density is $n = PN_A/RT$, where P, R, T, and N_A have their usual meanings, and thus, the mean-free path $\lambda_{mfp} \approx (nd_c^2\pi)^{-1} \approx 6$ μm, while the dimensions of the source boat and the pores of the grid are ∼1 cm and ∼30 μm, respectively. So the Knudsen numbers for the flow inside the Zn source boat and along the pores of the grid are $\sim 10^4$ and ∼3, respectively, indicating that near the grid the flow changes

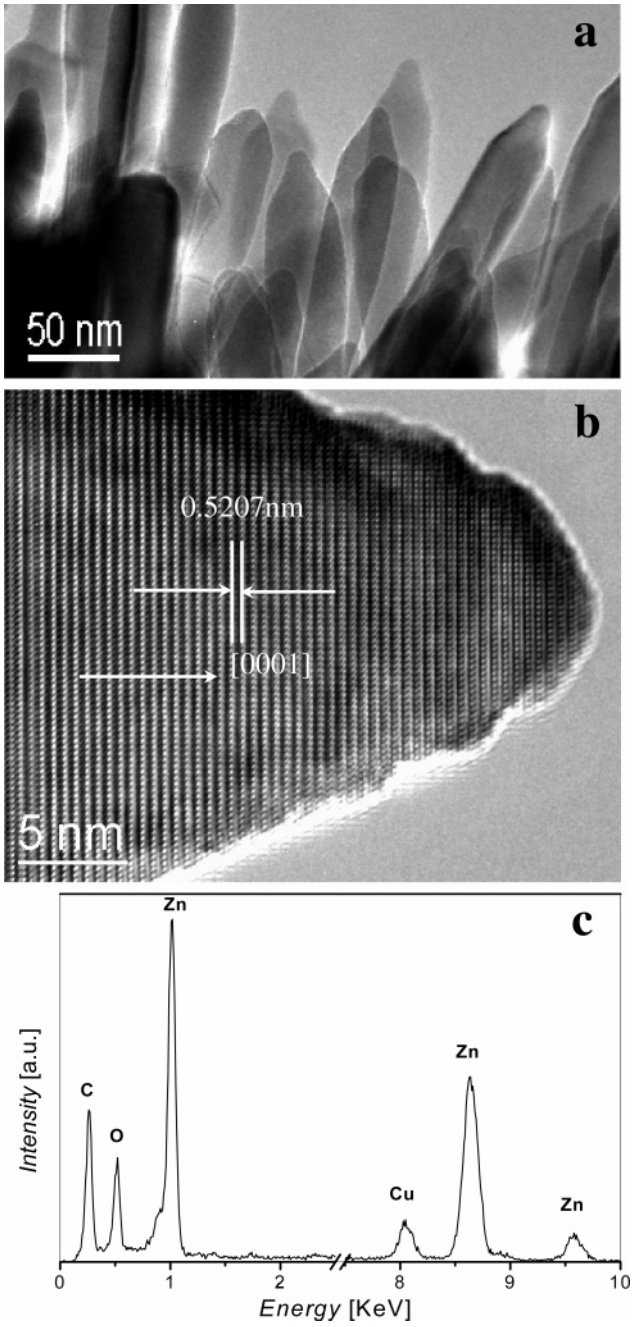

Figure 3. (a) TEM image of the ZnO nanorods with diameters of ~30 nm. (b) HREM image showing the tip of ~5 nm of a single nanorod and the growth direction along the [0001] axis. (c) EDS analysis of a single nanowire.

from viscous to molecular flow. Therefore, the velocities of the impinging atoms on the Au-coated grid surface have significant vertical components, which could be a reason for the good alignment of the samples. In the case of the conventional CVD (CVT), the gas flow adjacent to the substrate surfaces is parallel to the surfaces, and thus, a poor alignment is normal for samples grown via CVD. In addition to the good alignment, the selective growth of the ZnO nanorod arrays can be fulfilled by designing the shape of the grid. However, two problems are still not fully solved in this work. First, the function of Se is unclear, although it is a key factor for the morphology of the samples. Se species are not observed in the nanorods but only in the form of ZnSe nanoparticles covering some part of the grid. How to integrate the method to conventional Si technologies may be the other problem.

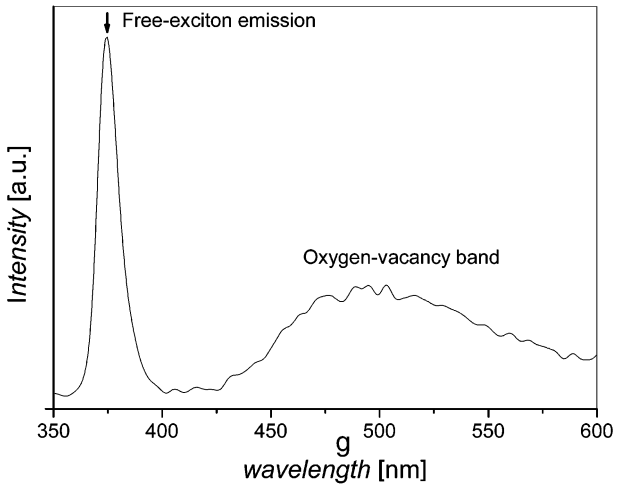

Figure 4. Room-temperature photoluminescence spectra exhibiting a strong UV peak at 3.31 eV and a weak green band in the range of 2.07−2.92 eV, which can be assigned to free-exciton and oxygen-vacancy emission, respectively.

Conclusion

In conclusion, the patterned growth of ZnO nanorod arrays has been realized on a stainless steel grid substrate. The as-grown nanorods were uniform in dimension with large aspect ratios and tiny tips. The grid-directed patterning of ZnO nanorod arrays on a supporting substrate offers a versatile method toward large-scale application such as high-efficiency filtering using nanostructured materials.

Acknowledgment. X.Y.X. and H.Z.Z. contribute equally to the work. This project is financially supported by the national 973 projects (No. 2002CB613505, MOST), National Natural Science Foundation of China (Grant Nos. 50025206, 60071014, 20151002), Scientific Research Foundation for the Returned Overseas Chinese Scholars, State Education Ministry, and 31st Postdoc Research Foundation. D.P.Y. acknowledges support from the Cheung Kong scholar program.

References and Notes

(1) Sberveglieri, G.; Groppelli, S.; Nelli, P.; Tintinelli, A.; Giunta, G. *Sens. Actuatuors, B* **1995**, *24*, 599.
(2) Chow, T. P.; Tyagi, R. *IEEE Trans. Electron Devices* **1994**, *41*, 1481.
(3) Ohta, H.; Kawamura, K.; Orita, M.; Sarukura, N.; Hirano, M.; Hosono, H. *Electron. Lett.* **2000**, *36*, 984.
(4) Yumoto, H.; Inoue, T.; Li, S. J.; Sako, T.; Nishiyama, K. *Thin Solid Films* **1999**, *38*, 345.
(5) Lee, S. S.; Ried, R. P.; White, R. M. *J. Microelectromech. Syst.* **1996**, *5*, 238.
(6) Mitra, A.; Thareja, R. K. *J. Appl. Phys.* **2001**, *89*, 2025.
(7) (a) Lee, J. S.; Kang, M.; Kim, S.; Lee, M.; Lee, Y. *J. Cryst. Growth* **2003**, *249*, 201. (b) Yao, B. D.; Chan, Y. F.; Wang, N. *Appl. Phys. Lett.* **2002**, *81*, 757.
(8) Huang, M. H.; Wu, Y.; Feick, H.; Tran, N.; Weber, E.; Yang, P. *Adv. Mater.* **2001**, *13*, 113.
(9) Heo, Y. W.; Varadarajan, V.; Kaufman, M.; Kim, K.; Norton, D. P.; Ren, F.; Fleming, P. H. *Appl. Phys. Lett.* **2002**, *81*, 3046.
(10) Kong, Y. C.; Yu, D. P.; Zhang, B.; Fang, W.; Feng, S. Q. *Appl. Phys. Lett.* **2001**, *78*, 407.
(11) Zhong, J.; Muthukumar, S.; Chen, Y.; Lu, Y.; Ng, H. M.; Jiang, W.; Garfunkel, E. L. *Appl. Phys. Lett.* **2003**, *83*, 3401.
(12) Saito, N.; Haneda, H.; Sekiguchi, T.; Ohashi, N.; Sakaguchi, I.; Koumoto, K. *Adv. Mater.* **2002**, *14*, 418.
(13) Li, Y.; Meng, G. W.; Zhang, L. D.; Phillipp, F. *Appl. Phys. Lett.* **2000**, *76*, 2011.
(14) Hung, C. H.; Whang, W. T. *J. Cryst. Growth* **2004**, *268*, 242.
(15) Yan, M.; Zhang, H. T.; Widjaja, E. J.; Chang, R. P. H. *J. Appl. Phys.* **2003**, *94*, 5240.

(16) Dong, L.; Jiao, J.; Tuggle, D. W.; Petty, J. M.; Elliff, S. A.; Coulter, M. *Appl. Phys. Lett.* **2003**, *82*, 1096.
(17) Zhu, Y. W.; Zhang, H. Z.; Sun, X. C.; Feng, S. Q.; Xu, J.; Zhao, Q.; Xiang, B.; Wang, R. M.; Yu, D. P. *Appl. Phys. Lett.* **2003**, *83*, 144.
(18) Vanheusden, K.; Warren, W. L.; Seager, C. H.; Tallant, D. K.; Voigt, J. A.; Gnade, B. E. *J. Appl. Phys.* **1996**, *79*, 7993.
(19) Ohring, M. *The Material Science of Thin Films*; Academic Press: New York, 1991.